J. Fluid Mech. (1999), *vol.* 394, *pp.* 97–117. Printed in the United Kingdom

© 1999 Cambridge University Press

Turbulence modification by particles in a backward-facing step flow

By JOHN R. FESSLER AND JOHN K. EATON

Department of Mechanical Engineering, Stanford University, Stanford, CA 94305, USA

(Received 1 June 1998 and in revised form 16 February 1999)

The current study investigates turbulence modification by particles in a backward-facing step flow with a fully developed channel flow inlet. This flow provides a range of flow regimes in which to compare turbulence modification under the same experimental conditions. Gas-phase velocities in the presence of 3–40% mass loadings of three different particle classes (90 and 150 μm diameter glass and 70 μm diameter copper spheres) were measured. Attenuation of the streamwise fluid turbulence of up to 35% was observed in the channel-flow extension region of the flow for a 40% mass loading of the largest particles. The level of attenuation decreased with decreasing particle Stokes number, particle Reynolds number and mass loading. No modification of the turbulence was found in the separated shear layer or in the redevelopment region behind the step, although there were significant particle loadings in these regions.

1. Introduction

The interactions between small, dense particles and gas-phase turbulence are extremely complex and, despite the importance of numerous industrial and natural particle-laden flows, many of the interactions remain poorly understood. Only a few aspects, such as particle dispersion in homogeneous flows, can be investigated analytically. Real particle-laden flows are usually inhomogeneous and anisotropic, often include wall interactions or flow separation, and are subject to instabilities that produce large-scale structure which varies markedly from flow to flow. One problem area which bars successful prediction of complex particle-laden flows is the modification of the gas-phase turbulence by the particles. The present work examines this effect in a single-sided, planar sudden expansion, a geometrically simple flow which contains many of the important features of more complex industrial and natural flows.

It is now well known that moderate mass loadings of fine particles can create very signficant changes in the turbulence levels in the flow. Reviews by Hetsroni (1989) and Gore & Crowe (1991) established that, in general, small particles can attenuate fluid turbulence, while large particles can augment it. Gore & Crowe (1991) identified the ratio of the particle diameter to a characteristic eddy length scale as the parameter that determines the effect of the particles on the fluid turbulence, while Hetsroni (1989) found the particle Reynolds number to be the appropriate parameter. Neither identified the parameters which govern the degree of turbulence modification. Restricting ourselves to the regime of small, dense particles, which attenuate turbulence, some of the relevant parameters for turbulence modification are becoming apparent. In wall-bounded flows, the pipe flow studies of Maeda, Hishida & Furutani (1980), Tsuji & Morikawa (1982) and Tsuji, Morikawa & Shiomi (1984), the two-dimensional boundary layer study of Rogers & Eaton (1991) and

https://doi.org/10.1017/S0022112099005741 Published online by Cambridge University Press

the fully developed channel flow study of Kulick, Fessler & Eaton (1994) all found that turbulence attenuation increases with both mass loading and particle Stokes number. The latter trend contradicts the current particle-laden flow models where 'extra dissipation due to particles' is inversely proportional to particle time constant (cf. Elghobashi & Abou-Arab 1983; also, see Squires & Eaton 1994 for a review of numerous K–ϵ particle laden flow models.) The situation is not as well resolved in simple free shear flows. Yang *et al.* (1990) showed analytically that Kelvin–Helmholtz rollers form more slowly in particle-laden flow. However, the study of Longmire & Eaton (1990) found that mass loadings as large as 80% had little effect on vortex rings in an axisymmetric jet. Mostafa *et al.* (1989) and Hishida *et al.* (1989) found turbulence attenuation in free shear layers for particle mass loadings greater than 20%. Due to the differences in loading and measurement techniques used in the various studies, it has been hard to directly compare results to discern trends other than an increase of attenuation with increasing mass loading. Squires & Eaton (1990) and Elghobashi & Truesdell (1993) used direct numerical simulation to examine turbulence modification in isotropic turbulence. Squires & Eaton forced the simulations to maintain stationarity, finding attenuation that was nearly constant with changes in Stokes number. Elghobashi & Truesdell (1993) found changes in the turbulence decay rate that were dependent on several factors including the gravitational field strength.

Maeda, Kiyota & Hishida (1982) and Hishida & Maeda (1991) investigated a backward-facing step flow with a 50% loading of 45 μm diameter glass particles. Both of the studies found reduction in the turbulent fluctuations along the dividing streamline but little modification in the free stream or after the reattachment point. Hardalupas, Taylor & Whitelaw (1992) investigated axisymmetric sudden expansions with 23% and 86% mass loadings of 80 μm diameter glass particles. In the near field, the turbulent fluctuations were reduced, but further downstream, modification to the mean flow led to increased turbulence levels. These few studies do not provide sufficient information to evaluate all the factors affecting turbulence modification in sudden expansion flows.

The present study investigated a particle-laden backward-facing step with a fully developed channel flow inlet. This flow is ideal for studying particle–turbulence interactions because the channel mean flow statistics are known to be unchanged by the presence of particles (Kulick *et al.* 1994). This was essential to ensure that any observed changes in the turbulence were due to the presence of particles, since separated flows are quite sensitive to the upstream mean velocity profile (see reviews of Eaton & Johnston 1980 and Simpson 1996). Also, turbulence modification is well documented in the fully developed channel flow, which provides a good baseline for comparison of the separated flow results. Downstream of reattachment, the flow should eventually return to fully developed channel flow, again providing a known asymptote for the results. An important feature of the present study was that the particle mass loading, Stokes number, and Reynolds number were all varied holding all other factors constant.

The specific objectives of the work reported here were to investigate modification of the gas-phase turbulence and the particle response in the separated, reattaching, and redeveloping regions of the backward-facing step. The study used three different particle classes, 90 and 150 μm diameter glass particles, and 70 μm diameter copper particles which provided two different particle Stokes numbers and three different particle Reynolds numbers. Gas-phase velocities in the presence of particles were measured for mass loadings ($\dot{m}_p/\dot{m}_{air}$) of these particles from 3% to 40%.

https://doi.org/10.1017/S0022112099005741 Published online by Cambridge University Press

Channel flow:		Backward-facing step flow:	
Channel half-width, h	20 mm	Step height, H	26.7 mm
Channel span	457 mm	Expansion ratio	5 : 3
Centreline velocity, U_0	10.5 m s^{-1}	Aspect ratio	17 : 1
$Re_h = \frac{U_0 h}{\nu}$	13 800	$Re_H = \frac{U_0 H}{\nu}$	18 400
u_τ, friction velocity	0.5 m s^{-1}	τ_f, large eddy time scale, $\frac{5H}{U_0}$	12.7 ms
Viscous length scale	31 μm		
Dissipation, ϵ, centreline (est.)	4.3 m^2 s^{-3}		
Kolmogorov length scale, η, centreline (est.)	170 μm		

TABLE 1. Flow parameters.

2. Experimental facility and techniques

2.1. *Flow field*

The flow was a single-sided sudden expansion oriented vertically downward to avoid complications due to particle settling. The Reynolds number of the inlet channel flow was 13 800, based on the centreline velocity of 10.5 m s^{-1} and the channel half-height, and the Reynolds number of the backstep, based on channel centreline velocity and step height was 18 400. The Reynolds number of the channel flow corresponded to the previous work of Kulick *et al.* (1994) to facilitate comparison between the two studies. The expansion ratio was $\frac{5}{3}$, which matches a single-phase study by Eaton & Johnston (1980). The aspect ratio of the sudden expansion (width/step height) was 17 : 1, which was sufficient to ensure essentially two-dimensional flow throughout a significant portion of the test section.

The inlet flow conditioning, flow exhaust and particle feeding systems were the same as used in the channel flow study of Kulick *et al.* (1994) and are illustated in figure 1. This system provided uniform fluid velocity and particle loading at the inlet of the development section. A 5.2 m long channel flow development section ensured fully developed flow at the inlet to the test section and allowed sufficient time (at least three particle time constants in the worst case) for the particles to come to equilibrium with the channel flow. The blower speed was controlled to supply a constant mass flow of air while the particle mass flow was varied from case to case. Additional information on the flow field is provided in table 1.

2.2. *Particle description*

Three classes of particles were used: 90 μm glass, 150 μm glass and 70 μm copper spheres. The size distribution of each particle class was determined through Coulter Counter size measurements. The 150 μm glass and 70 μm copper were chosen to have the same Stokes number while having different particle Reynolds numbers and the 90 μm glass particles provided a third set with a smaller Stokes number and an intermediate Reynolds number.

The Reynolds number characterizing the particle motion is defined as

$$Re_p = \frac{d_p U_{rel}}{\nu}, \tag{1}$$

where d_p is the particle diameter, ν is the fluid kinematic viscosity, and U_{rel} is a velocity

https://doi.org/10.1017/S0022112099005741 Published online by Cambridge University Press

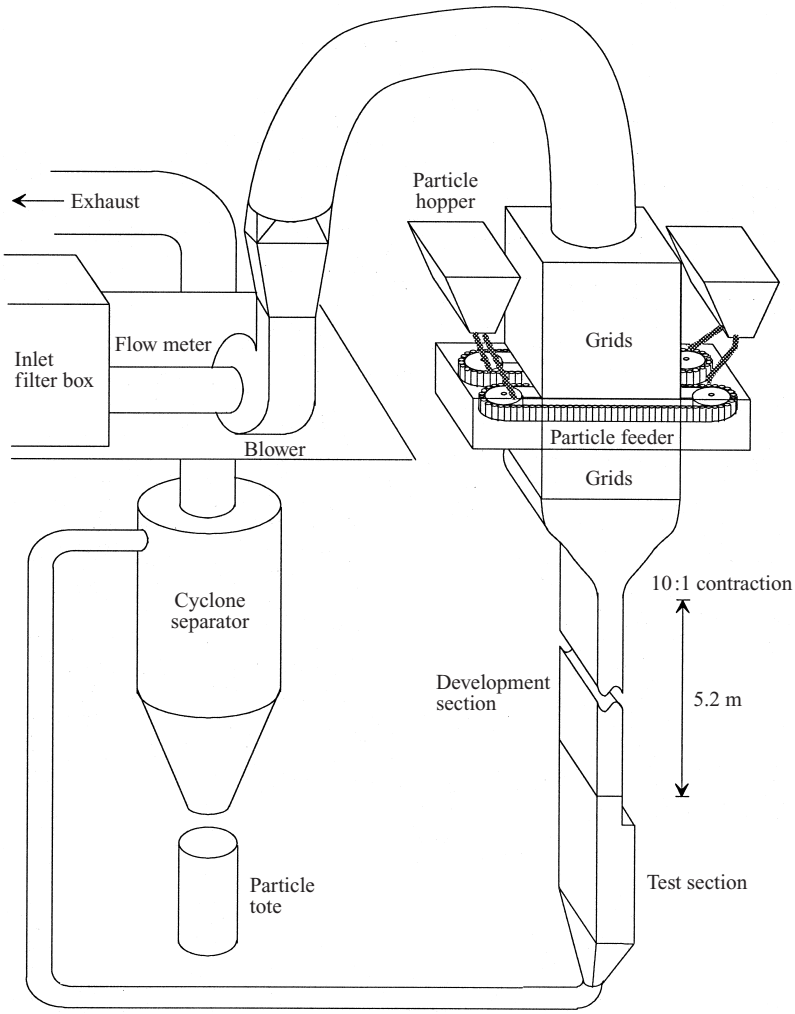


FIGURE 1. Schematic of experimental facility.

scale characterizing the average particle slip velocity relative to the flow. A number of velocity scales may be appropriate to characterize the average particle slip velocity, including the particle–fluid mean velocity difference, the terminal velocity of the particles, or the fluctuating particle or fluid velocities. Table 2 gives some representative ranges for these velocity scales and shows that there are wide variations in some of them. Fortunately, all of the scales are of the order of $1\,\mathrm{m\,s^{-1}}$, so choosing any one of the velocity scales as representative is appropriate. For the present experiment, it is perhaps best to choose the average fluctuating fluid velocity. All three particle sizes had relatively large Stokes numbers so they were not very responsive to the instantaneous fluid motion. Also, as will be seen, the mean slip velocity between the fluid and particles was small in most regions of the flow. Therefore, either the fluid or particle r.m.s. velocity is an appropriate scale for the instantaneous velocity difference. In the present flow, these values are similar with an average around $1.2\,\mathrm{m\,s^{-1}}$. This velocity value was thus chosen to compute the characteristic Reynolds number for all three particle classes.

https://doi.org/10.1017/S0022112099005741 Published online by Cambridge University Press

Velocity scale	Symbol	Range ($m\,s^{-1}$)
Particle–fluid mean velocity difference	$\|U - V\|$	0–1.0
Particle–fluid r.m.s. streamwise fluctuating velocity difference	$\|u' - v'\|$	0–1.1
Fluid r.m.s. streamwise fluctuating velocity	u'	0.4–1.8
Particle r.m.s. streamwise fluctuating velocity	v'	0.6–2.5
Terminal velocity, 90 μm glass	U_T	0.46
Terminal velocity, 150 μm glass	U_T	0.92
Terminal velocity, 70 μm copper	U_T	0.88

TABLE 2. Various velocity scales for particle Reynolds number definition.

The Stokes number is the ratio of the particle response time to a representative time scale in the flow,

$$St = \frac{\tau_p}{\tau_f}. \tag{2}$$

For small particles with negligible Reynolds numbers, Stokes (1851) showed that the particle time constant is

$$\tau_{p,Stokes} = \frac{(2\rho_p + \rho_f)d_p^2}{36\mu}. \tag{3}$$

For solid particles in a gaseous medium, the effect of the fluid density will be negligible and the Stokesian time constant will reduce to

$$\tau_{p,Stokes} = \frac{\rho_p d_p^2}{18\mu}, \tag{4}$$

where ρ_p is the particle density, d_p is the particle diameter and μ is the fluid kinemetic viscosity. However, this time constant definition is strictly true only for creeping flow and modification of the particle time constant for non-negligible Reynolds number is necessary for the present particles. The drag coefficient, C_D, can be corrected for Reynolds numbers up to 700 by using the following relation:

$$C_D = \frac{24}{Re_p}[1 + 0.15Re_p^{0.687}] \tag{5}$$

(Torobin & Gauvin 1959). The increase in drag coefficient as Reynolds numbers increase will decrease the particle time constant so the modified time constant used in this study is

$$\tau_p = \frac{\tau_{p,Stokes}}{[1 + 0.15Re_p^{0.687}]}. \tag{6}$$

The fluid time scale chosen, τ_f, was based on an approximate large-eddy passing frequency in the separated shear layer,

$$\tau_f = \frac{5H}{U_0}, \tag{7}$$

where H is the step height and U_0 is the channel centreline velocity. Dominant frequencies on this order were found by single-phase spectral measurements and in the single-phase experimental studies of Eaton & Johnston (1980) and Bhattacharjee, Scheelke & Troutt (1986). More detailed information on the particle classes is provided in table 3.

https://doi.org/10.1017/S0022112099005741 Published online by Cambridge University Press

Nominal diameter (μm)	90	150	70
Material	glass	glass	copper
Number mean diameter (μm)	91.2	147.2	68.2
Stan. dev. of diameter (μm)	5.2	10.0	10.9
Density ($\mathrm{kg\,m^{-3}}$)	2500	2500	8800
Stokes mean particle time constant, $\tau_{p,Stokes}$ (ms)	61	167	130
Modified mean particle time constant, τ_p (ms)	38	92	88
Large-eddy Stokes number, St	3.0	7.2	6.9
Particle Reynolds number, Re_p	7.3	11.8	5.5

TABLE 3. Particle parameters.

2.3. *Experimental methods*

All velocities were measured using laser Doppler anemometry (LDA) which could measure the velocities of both very small, $O(1\,\mu\mathrm{m})$, titanium dioxide flow tracers and the large glass and copper particles. Each data point represents 2000 individual velocity samples which yields statistical uncertainties ranging from $\pm 0.02\,\mathrm{m\,s^{-1}}$ to $\pm 0.08\,\mathrm{m\,s^{-1}}$ on the mean velocities and $\pm 3\%$ on the measured standard deviations. To measure the velocity of the tracer particles in the presence of the large particles, a two-counter technique utilizing pedestal amplitude descrimination was employed. This method, shown schematically in figure 2, used one TSI Model 1980b counter processor to measure the velocity from the downmixed signal in the traditional manner. A second 1980b counter processor determined whether a particle was large or small using the pedestal information contained in the raw, undownmixed signal. This technique has been previously qualified in the study of Kulick *et al.* (1994) and found to produce very little particle–fluid crosstalk error through the combination of amplitude descrimination and a stringent fringe crossing requirement.

Although it is difficult to calculate directly the amount of crosstalk, it has been estimated, based on relative data rates before and after the addition of tracers, that less than 5% of the laden flow measurements came from large particles misrepresented as tracer particles. Crosstalk from particles can affect the laden flow statistics because the mean and standard deviation of the particle velocity distribution can be different than the corresponding laden flow statistics. As table 2 shows, the streamwise mean and fluctuating velocities can differ by as much as $1\,\mathrm{m\,s^{-1}}$. An estimate of the effect of crosstalk was made by constructing Gaussian velocity distributions for various conditions given the measured particle and laden velocity statistics. It was then assumed that 5% of the particle velocities were erroneously measured as laden velocities. For the worst case scenarios in the streamwise direction, 5% crosstalk would result in an overestimation of the mean laden velocity of 0.5% and an overestimation of the laden standard deviation of up to 20%. In other words, the reported measurements of laden standard deviation could represent 120% of the true values. Naturally, in areas where the particle and fluid statistics are closer in value, this error is significantly reduced. It should be noted, however, that for the streamwise direction, this error due to crosstalk would result in an underestimation of turbulence attenuation. In the wall-normal direction, the mean velocities of the fluid and particles are much closer together and an error in the mean of only $0.001\,\mathrm{m\,s^{-1}}$ is expected due to crosstalk. The particle velocity probability density functions (PDFs) for the wall-normal direction were narrower than the fluid velocity PDFs, so in this case, crosstalk error would tend to reduce the

https://doi.org/10.1017/S0022112099005741 Published online by Cambridge University Press

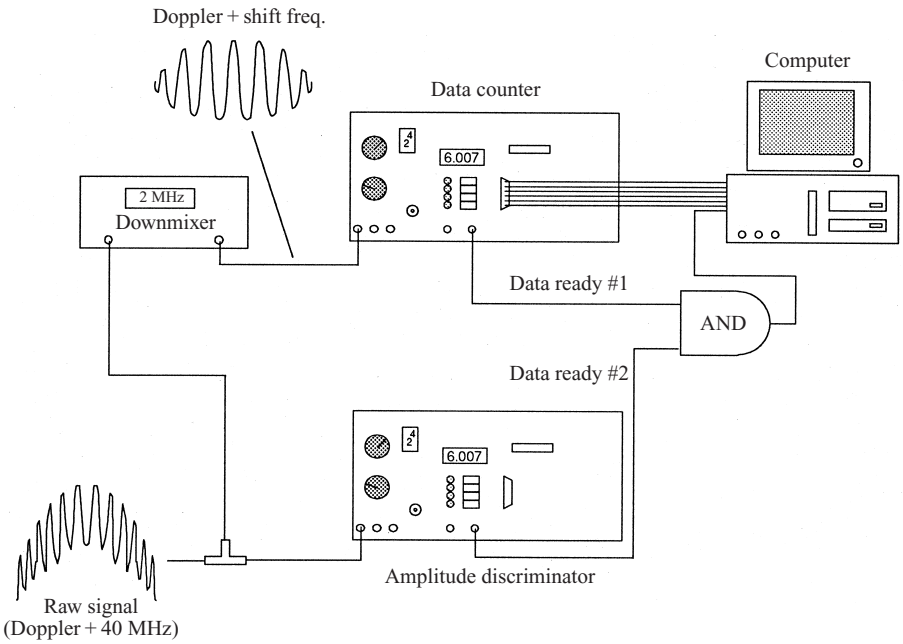


FIGURE 2. Schematic of two-counter technique for descriminating particle and gas velocities.

measured standard deviation, and thus overestimate turbulence attenuation, by up to 1.5%.

Mean particle number density fields were measured by illuminating the particles with a single pulse from a frequency-doubled, 10 mJ per pulse Neodimium: YAG laser and recording the images on black and white film. The photographs were scanned into a flat bed scanner and custom image processing software, described in Fessler, Kulick & Eaton (1994) identified each particle's size and location in the flow field. The entire flow field was imaged in two halves, from $x/H = 0$ to 7 and $x/H = 7$ to 14, and at least fifty individual photographs were averaged to obtain well resolved statistics.

3. Presentation and discussion of results

3.1. *Particle velocity data*

Mean and r.m.s. particle velocity profiles were measured for the experimental conditions shown in table 4(*a*). Few particles were found in the recirculation region directly behind the step, so no data are available near the wall for the stations at $x/H = 2, 5$, and 7. Figure 3 shows a contour plot of the mean particle number density for the 70 μm copper particles. The particle concentration measurements were virtually identical for the 150 μm glass and 90 μm glass beads. The figure shows that very few particles are found in the recirculation region. After the reattachment point ($x/H = 7.4$) increasing numbers of particles can be found below $y/H = 1$ until at $x/H = 14$ the number density across the section is becoming more uniform. The lack of particles in the recirculation region is not surprising because the Stokes numbers of the particles based on the large-eddy time scale, $\tau_f = 5H/U_0$, are all significantly larger than unity. Previous studies (see Hardalupas *et al.* 1992) have found that particles will be dispersed into the recirculation region only if their large-eddy Stokes

https://doi.org/10.1017/S0022112099005741 Published online by Cambridge University Press

		Streamwise direction		Wall-normal direction	
	Particle class	x/H	Mass loading	x/H	Mass loading
(*a*)	90 μm glass	2, 5, 7, 9, 14	20%	—	—
	150 μm glass	2, 5, 7, 9, 14	20%, 40%	2, 5, 7, 9, 14	10%
	70 μm copper	−2, 0, 2, 5, 7, 9, 12	3%, 10%	2, 5, 7, 9, 14	20%
(*b*)	90 μm glass	2, 5, 7, 9, 14	20%	—	—
	150 μm glass	2, 5, 7, 9, 14	20%, 40%	2, 5, 7, 9, 14	10%
	70 μm copper	−2, 0, 2, 5, 7, 9, 12	3%, 10%	—	—
	70 μm copper	2, 5, 7, 9, 14	20%, 40%	2, 5, 7, 9, 14	20%

TABLE 4. Parameter space for (*a*) particle and (*b*) gas-phase velocity profiles.

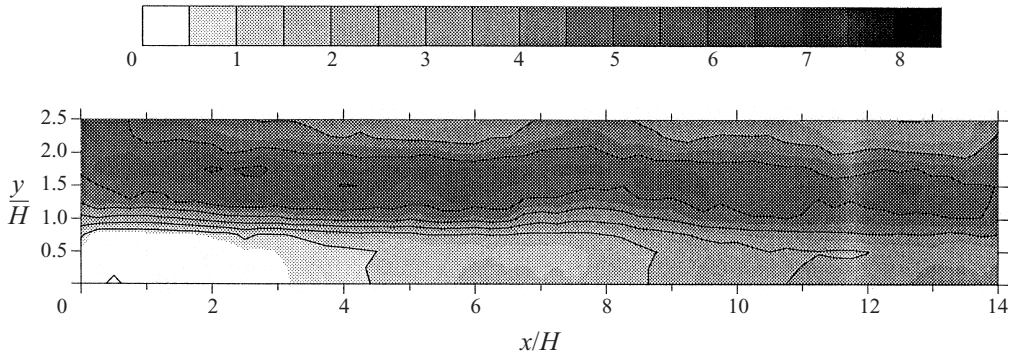


FIGURE 3. Contour plot of mean particle number density distribution for 70 μm copper particles.

numbers are less than one. Another parameter which may be important in this vertically downward flow is the ratio of the particle's terminal velocity to the maximum velocity of reverse flow, V_t/U_{rev}. The maximum reverse flow velocity found in this flow is approximately $0.2U_0$. The resulting ratios for the 70 μm copper, 150 μm glass and 90 μm glass particles are 0.44, 0.46 and 0.23 respectively. These ratios are all large enough that particles would have difficulty moving upstream (vertically upward) into the recirculation region.

Both streamwise and wall-normal velocities were measured for all three particle classes and reported in Fessler & Eaton (1995, 1997). A sample of the results for the 70 μm copper particles is shown here to illustrate the most important trends. The streamwise mean velocity profiles at five stations are shown in figure 4 compared to the unladen gas-phase velocity profiles. It will be shown below that the gas-phase mean velocity profiles are not significantly changed by particle loading except at the farthest downstream location, $x/H = 14$. At $x/H = 2$, the particle velocities are lower than the fluid velocities. This is a remnant of a phenomenon observed by Kulick *et al.* (1994) where the particles in the channel flow show a negative slip velocity due to cross-stream transport. Farther downstream, the particle velocities exceed the gas velocities due to the deceleration of the fluid in the sudden expansion. Mean particle velocities in the wall-normal direction (not shown) were generally similar to or slightly smaller than the corresponding fluid velocities.

https://doi.org/10.1017/S0022112099005741 Published online by Cambridge University Press

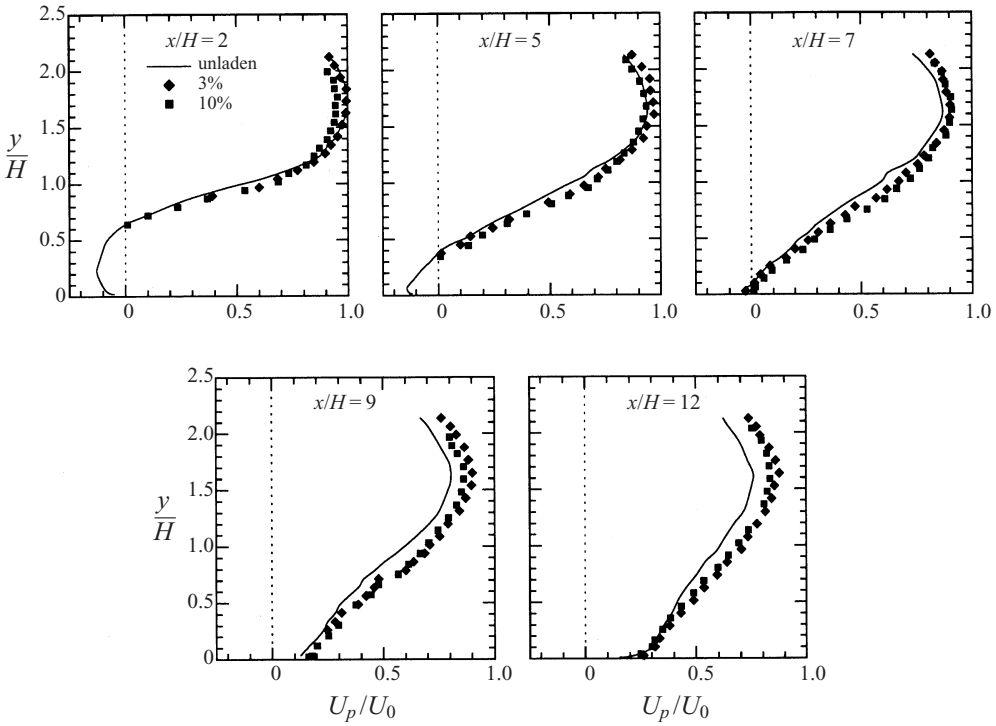


FIGURE 4. 70 μm copper particle streamwise mean velocities.

The streamwise r.m.s. velocity fluctuations of the particles are shown in figure 5. For the most part, the particles showed higher fluctuating velocities than the unladen gas. This phenomenon, also found in numerous previous studies, is a result of transport of inertial particles across regions of mean shear. The particles' r.m.s. fluctuating velocities in the wall-normal direction (figure 6) are consistently lower than the fluid, as expected for flow directions with low mean shear.

3.2. *Gas-phase velocities*

Measurements of the gas-phase statistics in the presence of particles (henceforth known as laden measurements) were acquired for the experimental conditions listed in table 4(*b*). For each case the mass flow of air through the system was held constant while the mass flow of particles was varied.

Figure 7 shows the laden streamwise mean velocity profiles with 70 μm copper particles compared to the unladen flow. No modification of the mean flow was observed in the upstream channel before the sudden expansion (not shown) or for the downstream stations between $x/H = 2$ and 9. Some retardation of redevelopment was observed in the farthest downstream location of $x/H = 14$. Similar results were found for all of the particle classes investigated. The results for the channel flow upstream of the sudden expansion agree with the results of Kulick *et al.* (1994) which showed no modification of the mean flow in a downward-flowing particle-laden channel flow. The lack of modification in the channel flow may be explained by the uniform body force acting on the particles. Because particles are uniformly distributed throughout the flow, the body force will act uniformly across the channel and simply reduce the pressure gradient required to balance the wall shear stress in fully developed flow.

https://doi.org/10.1017/S0022112099005741 Published online by Cambridge University Press

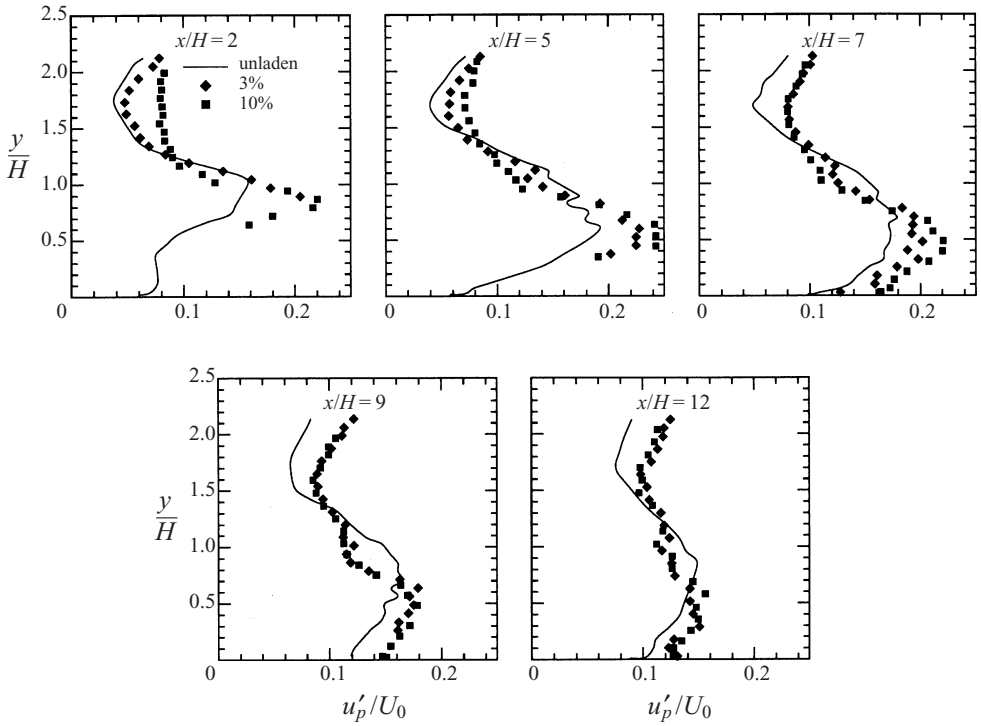


FIGURE 5. 70 μm copper particle streamwise fluctuating velocities.

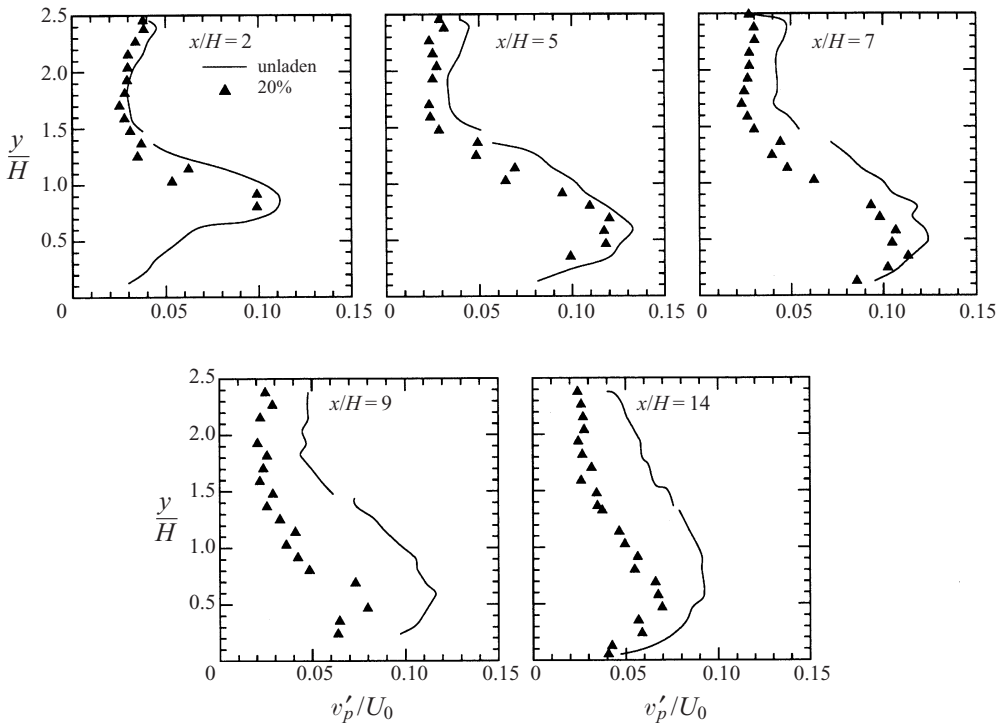


FIGURE 6. 70 μm copper particle wall-normal fluctuating velocities.

https://doi.org/10.1017/S0022112099005741 Published online by Cambridge University Press

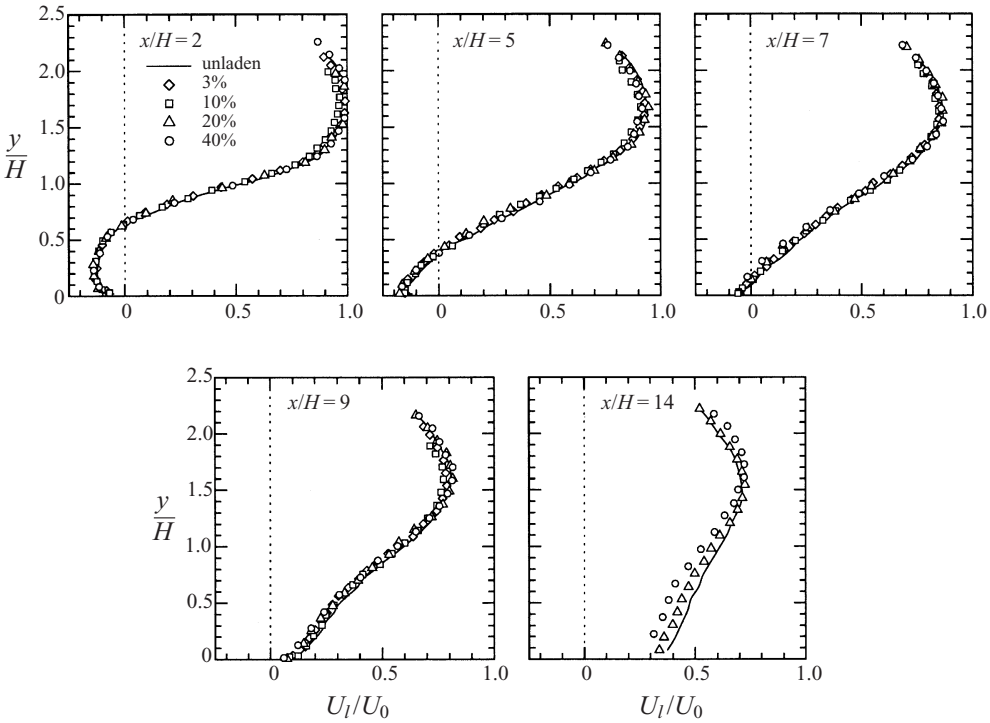


FIGURE 7. Mean streamwise gas-phase velocities in the presence of 70 μm copper particles.

In essence, the transfer of momentum from the particles to the fluid is acting as a replacement for some fraction of the pressure gradient. The effects of this momentum transfer should also be observed in the sudden expansion flow everywhere there are significant numbers of particles.

In the region before reattachment ($x/H = 2$–7.4) the laden gas flow is also found to be unmodified although particle number density surveys (see figure 3) show that very few particles are found in the recirculation region. Presumably the effect of the particles on the mean flow should be different in the regions with and without particles. However, in this region the pressure gradient is much stronger than that found in the fully developed channel. As a result the effects of momentum transfer from the particles in this region are overwhelmed by the very large pressure gradient. At the farthest downstream location, $x/H = 14$, the flow is well past the reattachment point and pressure gradient has reduced to the point that the effect of the non-uniform particle loading is begining to affect the mean laden velocity statistics. Because there are fewer particles near the wall after reattachment, there is less of a body force in this area and the flow is slower to redevelop back into a channel flow.

Profiles of the laden gas mean wall-normal velocities are shown in Fessler & Eaton (1995) but are omitted here for brevity. These velocities were small, with the maximum velocity on the order of 0.5 m s^{-1}, and any modifications were correspondingly small. In fact, any observed modifications were on the same order as the uncertainty in this region of low mean velocity and high fluctuating velocity.

Figures 8–10 show the streamwise laden gas r.m.s. velocities compared to the r.m.s. velocities in the unladen flow. The results from the 90 μm glass show no measurable change in the fluid turbulence due to the presence of particles. Again it should be

https://doi.org/10.1017/S0022112099005741 Published online by Cambridge University Press

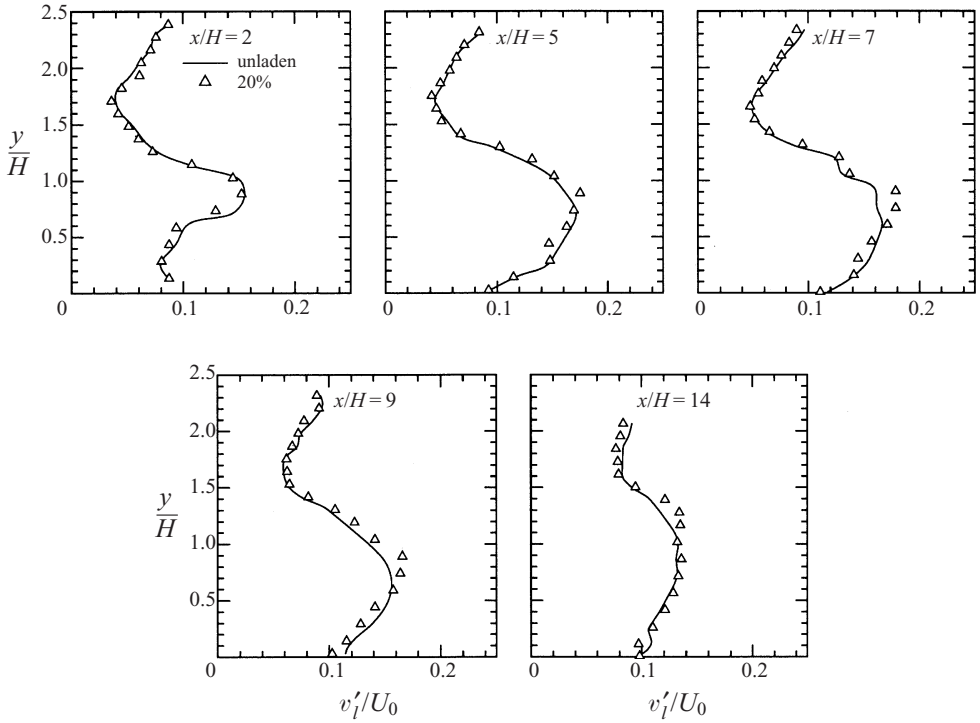


FIGURE 8. Fluctuating streamwise gas-phase velocities in the presence of 90 μm glass particles.

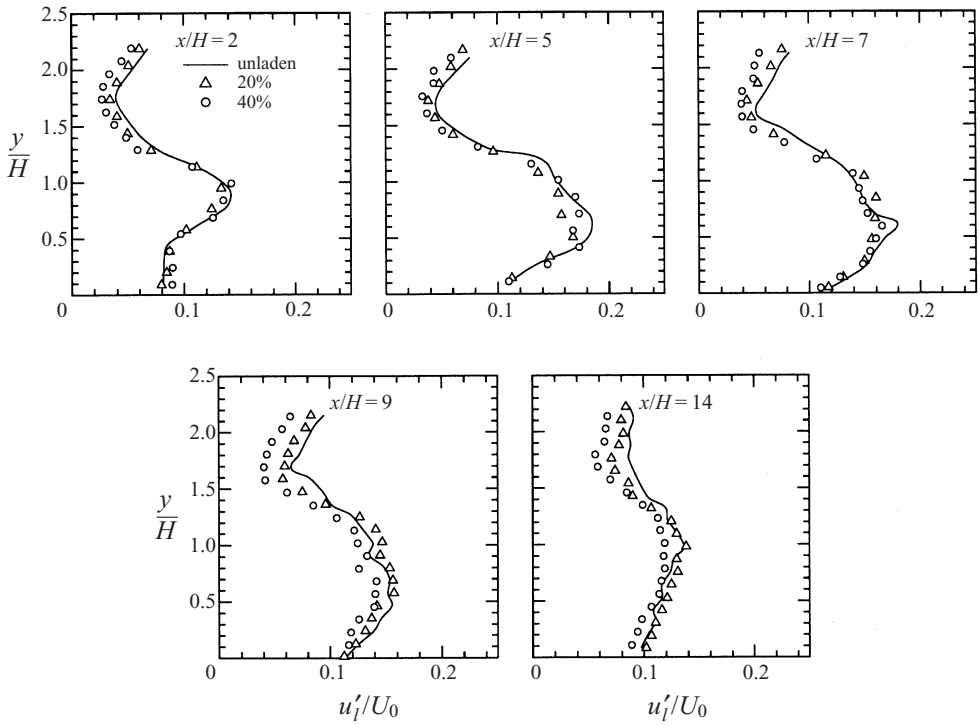


FIGURE 9. Fluctuating streamwise gas-phase velocities in the presence of 150 μm glass particles.

https://doi.org/10.1017/S0022112099005741 Published online by Cambridge University Press

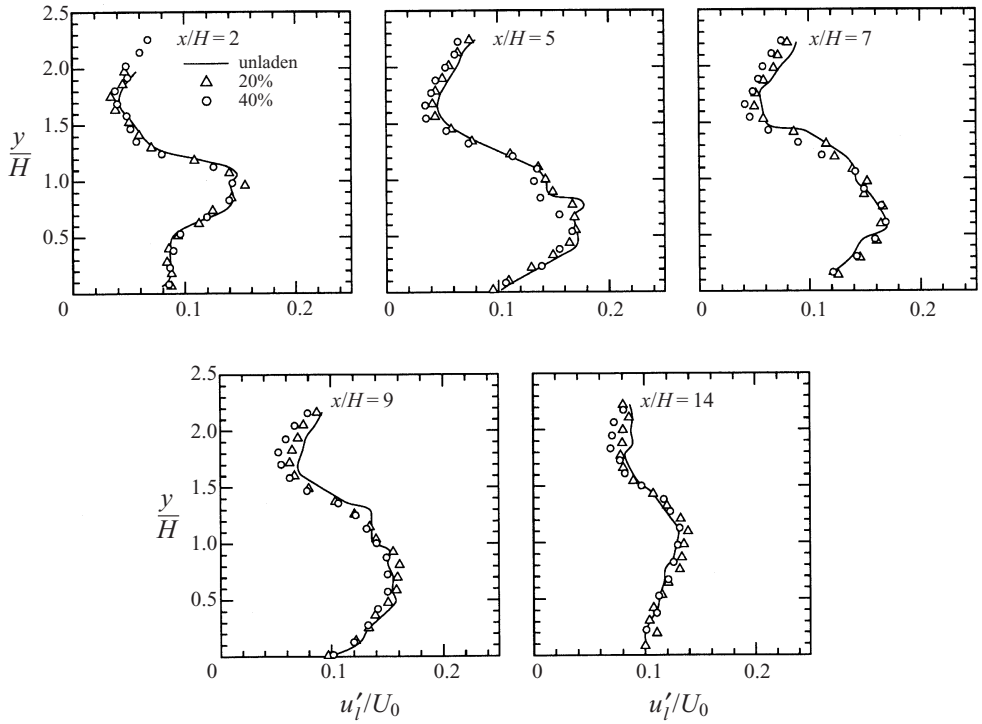


FIGURE 10. Fluctuating streamwise gas-phase velocities in the presence of 70 μm copper particles.

emphasized that these results are conservative in nature because particle crosstalk would serve only to increase measured gas-phase r.m.s. velocities. In these cases, there may be a small degree of turbulence attenuation which is masked by particle crosstalk. The higher mass loadings of the large Stokes number 70 μm copper and 150 μm glass particles do, however, show distinct turbulence attenuation for $y/H > 1$. The 150 μm glass particles show the largest attenuation with reductions in the turbulence of as much as 35% for a 40% mass loading. The turbulence in the shear layer and the recirculation zone is relatively unaffected by the particles. The particle number density fields (figure 3) indicate that while there are few particles in the region $y/H < 1$ before the reattachment point, significant spreading of the particles has occurred by the locations of $x/H = 9$ and 14. Thus the lack of turbulence modification is not simply a result of a lack of particles in the shear layer but rather a difference in the response of the turbulence in that region to the presence of particles.

Figures 11 and 12 show the profiles of the laden wall-normal fluctuating velocities. The profiles show the same trends as the streamwise data, with modification of the turbulence only for $y/H > 1$. The magnitudes of the modification at a given mass loading were also similar for the streamwise and wall-normal directions. Unfortunately optical constraints severely limited the mass loadings for which measurements could be made in the wall-normal direction, so less information is available to evaluate the effects of the relevant parameters on turbulence attenuation.

Figures 13(*a*)–13(*c*) show the ratio of the laden to unladen streamwise r.m.s. fluctuating velocity taken at the same location without changing air flow rate. These figures show the cases with 150 μm glass particles at streamwise locations of $x/H = 2, 7$

https://doi.org/10.1017/S0022112099005741 Published online by Cambridge University Press

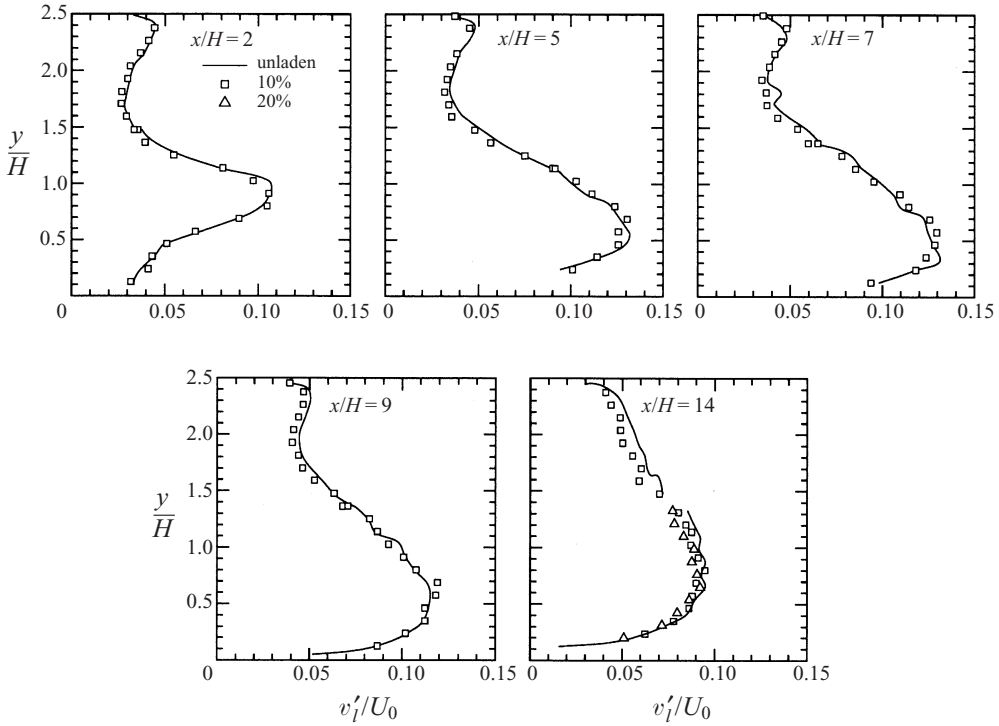


FIGURE 11. Fluctuating wall-normal gas-phase velocities in the presence of 150 μm glass particles.

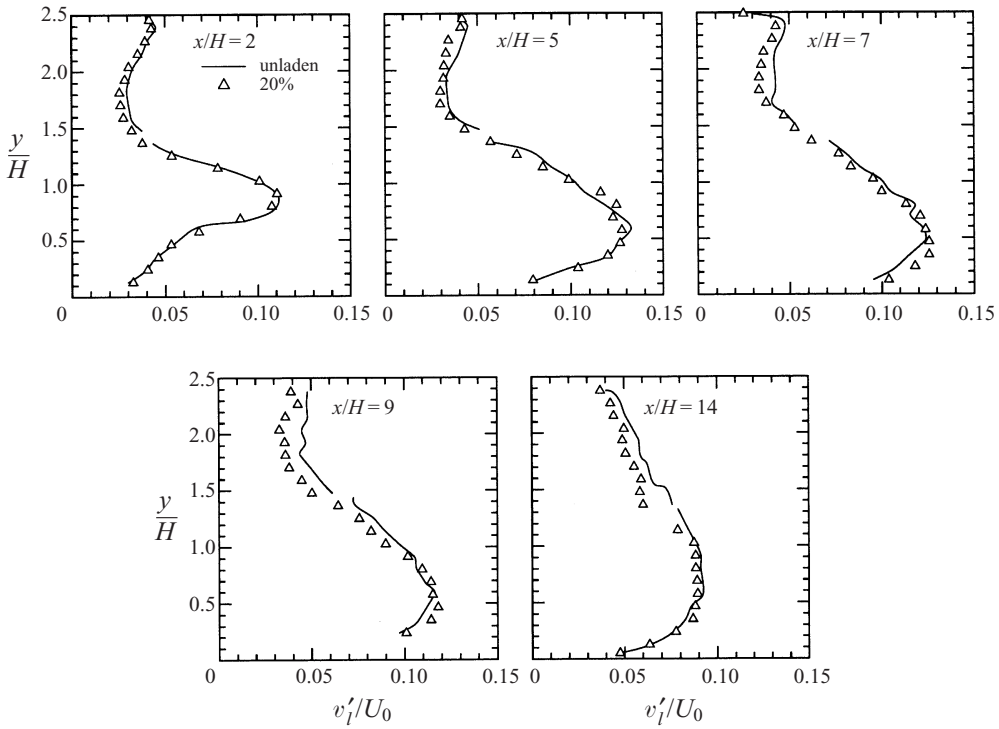


FIGURE 12. Fluctuating wall-normal gas-phase velocities in the presence of 70 μm copper particles.

https://doi.org/10.1017/S0022112099005741 Published online by Cambridge University Press

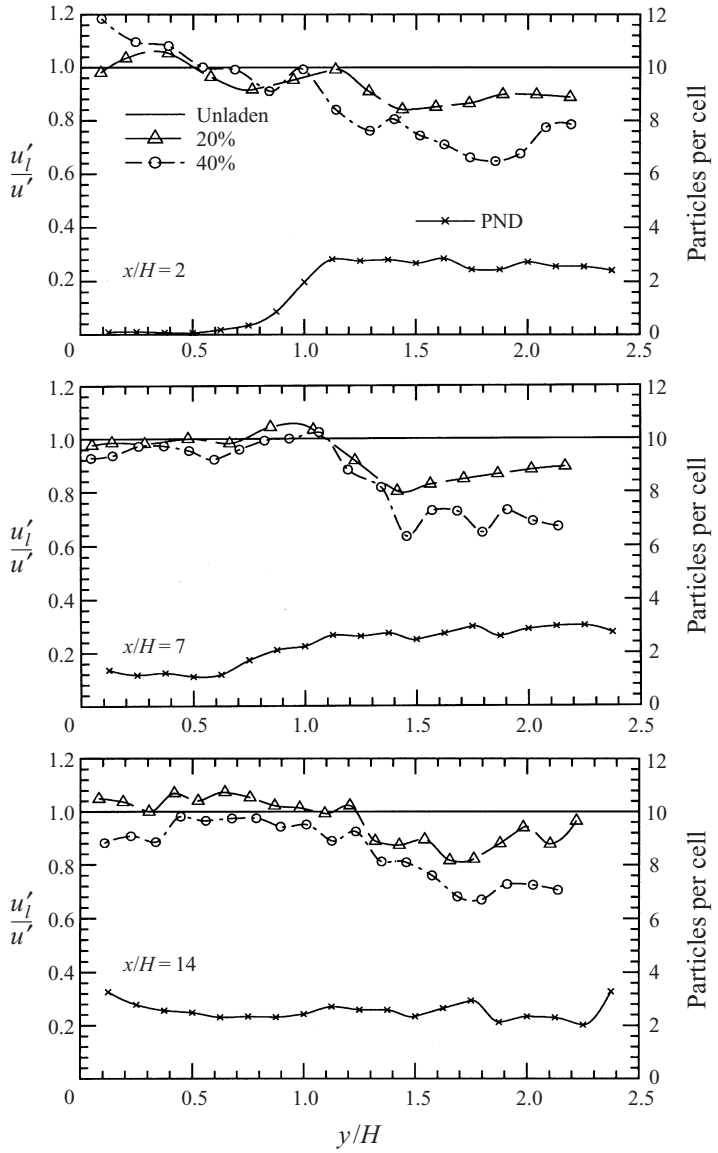


FIGURE 13. Ratio of laden to unladen fluctuating velocities in the presence of 150 μm glass particles and particle number density (PND).

and 14. In these ratio plots, any change in the turbulence due to the presence of particles will appear as a departure of the ratio from unity. Significant scatter is apparent in these plots as they are the ratio of two quantities which each have uncertainty on the order of $\pm 3\%$. Consequently any variations on the order of $\pm 5\%$ should be considered insignificant. Profiles of the particle number density, calculated from the laser sheet images are also shown for each specific streamwise location.

The plots show attenuation of up to 35% for a mass loading of 40% in the region $y/H > 1$. At x/H locations of 2 and 7 there are considerably more particles in the region of $y/H > 1$ but at $x/H = 14$ the particles have spread to fill the channel almost uniformly. Despite this fact, the turbulence attenuation is still small

https://doi.org/10.1017/S0022112099005741 Published online by Cambridge University Press

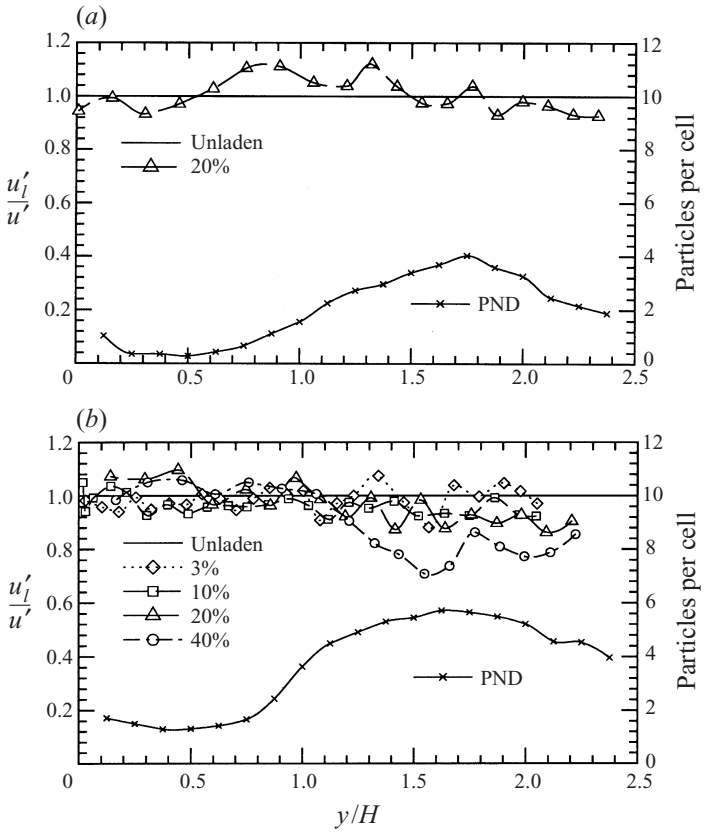


FIGURE 14. Ratio of laden to unladen fluctuating velocities in the presence of (*a*) 90 μm glass particles ($St = 3.0$ and $Re_p = 7.3$) and (*b*) 70 μm copper particles ($St = 6.9$ and $Re_p = 5.5$), and particle number density at streamwise location of $x/H = 7$.

for $y/H < 1$. It is known from previous studies on single-phase backward-facing steps that large-scale vortices persist far downstream of the reattachment point. It may be that the particles are simply much less effective at modifying the turbulence produced by these large-scale, energetic eddies.

Figures 14(*a*) and 14(*b*) show similar ratio plots for the other two particle classes at a streamwise location of $x/H = 7$. Comparison of these plots enables evaluation of the effects of particle Stokes number and Reynolds number on the degree of turbulence modification. The 70 μm copper and 150 μm glass particles have the same Stokes number ($St \approx 7$) but particle Reynolds numbers of 5.5 and 11.8 respectively. While the 150 μm glass particles show as much as 35% attenuation for a 40% loading, the 70 μm copper particles show only 25% attenuation for the same 40% loading. This indicates that the particle Reynolds number may also be a factor in determining the degree of turbulence modification. The 90 μm glass particles ($St = 3.0$ and $Re_p = 7.3$) show the least attenuation of all the particle classes as would be expected given their small Stokes number. Although previous studies (Hetsroni 1989) have shown that the Reynolds number is a factor in determining the sign of the turbulence modification, this study has shown that at a given particle Stokes number the particle Reynolds number can affect the degree of modification as well. This indicates that the change in particle wake structure with Reynolds number is important in determining the level of turbulence modification.

https://doi.org/10.1017/S0022112099005741 Published online by Cambridge University Press

For flows with a large ratio of particle to fluid material density and particle diameters smaller than the Kolmogorov scale, the particle path, the relative velocity, and the drag applied to the fluid are all uniquely determined by the particle time constant or Stokes number. The fact that two sets of particles with the same time constant but different particle Reynolds number produce different turbulence modification indicates that turbulence modification is not solely determined by the net interphase momentum transfer. Details of the flow distortion caused by the particles must play some role in determining the overall turbulence modification. Recent calculations by Eaton, Paris & Burton (1999) have shown that the flow distortion around the particle is a strong function of Reynolds number when the Reynolds number is of order 10, as it is in the present flow. The flow distortion is localized to a nearly symmetric region extending a few particle diameters at $Re_p = 1$, but by $Re_p = 10$ a strong asymmetry develops with the wake distortion extending many particle diameters downstream. Therefore, it is feasible that particles with diameters somewhat smaller than the Kolmogorov scale could actually distort small to moderate scale turbulent eddies.

4. Analysis and discussion

One of our main objectives in this study was to extend the knowledge gained from turbulence modification studies on simple flows to a more complex flow field with a variety of turbulence production mechanisms. From the study of Kulick *et al.* (1994) it is known that moderate mass loadings of small, dense particles can reduce the intensity of the gas-phase velocity fluctuations in the channel flow. The degree of modification increased with both particle mass loading ratio and Stokes number. The current study investigated the same parameters in the backward-facing step flow field and found the same trends to continue in certain regions of the flow. Turbulence modification similar to that found in the channel flow was found in the region of the channel flow extension ($y/H > 1$). This modification also increased with both particle mass loading and Stokes number. At these low mass loadings (less than 50%), turbulence attenuation appears to scale almost linearly with mass loading. The current study also investigated two particles with similar Stokes numbers but different particle Reynolds numbers and found that the degree of attenuation also increased with particle Reynolds number. The trend of increasing attenuation with particle Reynolds number cannot, however, continue indefinitely, as numerous previous studies (see the review of Hetsroni 1989) have found that particles with Reynolds numbers greater than 400 will enhance the turbulence in the flow. The existence of this limiting case suggests that there is some range of Reynolds numbers which results in maximum turbulence attenuation at a given Stokes number.

The turbulence levels were unchanged in the recirculation region, the separated shear layer, and the recovery region for $y/H < 1$. There were very few particles in the recirculation region so it was not surprising that there was no attenuation. However, there was a substantial loading in the separated shear layer and the particle loading in the recovery region was nearly uniform. The differences in level of attenuation may be due to differences in the turbulence time scale between the separated and reattaching flow and the channel flow. Table 5 gives representative large-scale and k/ϵ time scales for the centreline of the upstream channel flow and the shear layer. The large-scale time scales for the shear layer and channel centreline are 13 and 4 ms, respectively. (The large-scale time scale for the shear layer is based on $5H/U_0$, where H is the step height and U_0 is the centreline velocity. The channel flow has a wide range of turbulence scales, with the largest scales on the order of $2h/U_0$, where h is

https://doi.org/10.1017/S0022112099005741 Published online by Cambridge University Press

Flow regime	Large-eddy time scale (ms)	k/ϵ Time scale (ms)
Upstream channel flow centreline	4	45
Shear layer	13	14

TABLE 5. Time scales for channel flow and shear layer.

the channel half-width.) Because the fluid time scale is shorter in the channel flow, the particles in that region have higher Stokes number than those in the shear layer. Turbulence attenuation in the channel flow has been observed to increase with particle Stokes number (Kulick *et al.* 1994) so the observed spatial variations in turbulence attenuation may be a result of local Stokes number variations. On the other hand, if one looks at the time scale k/ϵ a different trend is observed in the two regions. At the inlet channel flow centreline k/ϵ is 45 ms and in the shear layer k/ϵ is 14 ms. This would indicate higher local Stokes numbers in the shear layer which should lead to higher turbulence attenuation, exactly the opposite of what was observed in this study. (The value of k/ϵ for the channel flow was computed using the $k-\epsilon-v^2$ model of Durbin 1991 and k/ϵ for the shear layer was found from the backward-facing step direct numerical simulation of Le & Moin 1994.) These conflicting results indicate that the local Stokes number is ill defined and not likely to be the crucial factor in determining turbulence attenuation.

A more likely mechanism to explain the spatial variation in turbulence attenuation is the difference in the magnitude of viscous dissipation between the two regions. The results of Le & Moin (1994) show that in the separated shear layer there is a broad peak in the production and dissipation near the dividing streamline. Outside the shear layer, in the channel flow extension, there will be relatively little production. Thus outside the shear layer, the equilibrium level of turbulent kinetic energy will largely be determined by the balance between turbulent transport and viscous dissipation, both of which are fairly small. In these regions a small change in the dissipation rate will result in a large change in the equilibrium turbulence level. An increase in dissipation of the same magnitude in the shear layer will only be a minor percentage change and will likely not affect the turbulence level significantly.

A third explanation for the differences in observed modification may be the residence time of the particles in the flow. In the channel flow extension region of the flow, the particles have had 5.2 m of development length in which to bring the turbulence level into equilibrium. After the sudden expansion, however, the particles have only 14 step heights (0.37 m) in which to affect the turbulence. Taking k/ϵ as a representative time scale for the cascade process through which the particles' effect on the flow is transported down to modifications in ϵ, and a representative velocity of 8 m s^{-1}, one finds that the particles need to be in the flow for approximately 0.1 m before significant modification would be expected. This could explain why little modification is observed in the redevelopment region where there are significant numbers of particles that have only recently entered this region of the flow.

The results of this study and others on turbulence modification have significant implications for modelling of particle-laden flows. The turbulence kinetic energy (TKE) transport equation is

$$\frac{\mathrm{D}k}{\mathrm{D}t} = \frac{\mathrm{D}k}{\mathrm{D}t}\Big|_{singlephase} - \frac{\overline{C}}{\rho_f \tau_p}(\overline{u_i u_i} - \overline{u_i v_i}) - \frac{1}{\rho_f \tau_p}(\overline{c u_i u_i} - \overline{c u_i v_i}) - \frac{1}{\rho_f \tau_p}(\overline{U_i} - \overline{V_i})\overline{c u_i}. \quad (8)$$

https://doi.org/10.1017/S0022112099005741 Published online by Cambridge University Press

This equation is a modified version of that found in Elghobashi & Abou-Arab (1983) for negligible volume fraction of particles. The first term on the right includes all the terms normally included in the single-phase TKE transport equation. The remaining terms are collectively known as the 'extra dissipation due to particles', or ϵ_p. In this equation u_i, v_i and c represent the fluctuating fluid velocity, particle velocity and particle concentration, respectively. The last two terms of (8) can be eliminated if the particle concentration fluctuations are uncorrelated to the fluid velocity field. It has been found that in this flow (Fessler & Eaton 1997) and in numerous other studies (see review by Eaton & Fessler 1994) that only particles with Stokes numbers on the order of one are preferentially concentrated. The heavy particles which caused significant turbulence attenuation in this flow were not preferentially concentrated so their distribution should be uncorrelated with the velocity field. Thus the extra dissipation term reduces to

$$\epsilon_p = \frac{\overline{C}}{\rho_f \tau_p}(\overline{u_i u_i} - \overline{u_i v_i}). \tag{9}$$

For the large Stokes number particles used in the turbulence attenuation studies, the correlation between fluid and particle velocity fluctuations, $\overline{u_i v_i}$, will be nearly zero (Rouson, Eaton & Abrahamson 1997). So the extra dissipation takes on a very simple form:

$$\epsilon_p = \frac{\overline{C}}{\rho_f \tau_p}(\overline{u_i u_i}) = \frac{2Ck}{\rho_f \tau_p}. \tag{10}$$

Note that in this form the extra dissipation term is inversely proportional to the particle time constant and thus the Stokes number. The results of this study and others directly contradict this relation. Obviously the influence that particles have on the flow is not fully captured by ϵ_p. One possibility, which has been largely ignored by current particle-laden flow models, is that the single-phase terms in the turbulent kinetic energy equation, $\mathrm{D}k/\mathrm{D}t|_{singlephase}$, may also be altered by the presence of particles. While the single-phase terms are unaltered in form by the presence of particles, there is no assurance that their values will remain constant upon the addition of particles. Thus the constants used for modelling the single-phase terms may be a function of particle Stokes number, Reynolds number and mass loading. This would result from the particles changing the structure of the turbulence, which in turn leads to changes in the fluid dissipation. This conclusion is bolstered by the sensitivity of the turbulence modification to particle Reynolds number.

The present results indicate that the picture of turbulence modification by particles is extremely complex. The degree of attenuation has been found to depend on a number of factors including particle Reynolds number, Stokes number, mass loading and the specific flow regime. Even in simple flows, current models of particle-laden flows are unable to predict the levels of turbulence attenuation and the trend of increasing modification with particle Stokes number. The added complexity of different modification in different flow regimes should prove to be a further challenge to these models.

5. Summary and conclusions

The current study investigated turbulence modification in a particle-laden flow over a backward-facing step. The results show that the degree of modification to the gas phase is an increasing function of both the particle Stokes number and Reynolds number. In addition to these parameters, the flow regime was found to strongly affect the degree of turbulence modification. After the reattachment point, in the region

https://doi.org/10.1017/S0022112099005741 Published online by Cambridge University Press

behind the step, very little turbulence modification was observed, although the number density of particles in this region was the same as that in the channel flow extension where significant modification was found. The particles are not able to affect the turbulence as greatly behind the step, where the mechanics of the flow are largely governed by lingering effects from the free shear layer formed at the separation point.

The authors appreciate the sponsorship of the National Science Foundation through (Grant # CTS-9312496) and a graduate fellowship awarded to the first author.

REFERENCES

Bhattacharjee, S., Scheelke, B. & Troutt, T. R. 1986 Modification of vortex interactions in reattached separating flow. *AIAA J.* **24**, 623–629.

Durbin, P. 1991 Near-wall turbulence closure modeling without 'damping functions'. *Theor. Comput. Fluid Dyn.* **3**, 1–13.

Eaton, J. K. & Fessler, J. R. 1994 Preferential concentration of particles by turbulence. *Intl J. Multiphase Flow* **20** (Suppl.), 169–209.

Eaton, J. K. & Johnston, J. P. 1980 Turbulent flow reattachment: An experimental study of the flow and structure behind a backward-facing step. *Mech. Engng Dept. Rep.* MD-39. Stanford University, Stanford, California.

Eaton, J. K., Paris, A. D. & Burton, T. M. 1999 Local distortion of turbulence by dispersed particles. *AIAA Paper* 99-3643.

Elghobashi, S. E. & Abou-Arab, T. 1983 A two-equation model for two-phase flows. *Phys. Fluids* **26**, 931–938.

Elghobashi, S. E. & Truesdell, G. C. 1993 On the two-way interaction between homogeneous turbulence and dispersed solid particles. I: Turbulence modification. *Phys. Fluids* A **5**, 1790–1801.

Fessler, J. R. & Eaton, J. K. 1995 Particle-turbulence interaction in a backward-facing step flow. *Mech. Engng Dept. Rep.* MD-70. Stanford University, Stanford, California.

Fessler, J. R. & Eaton, J. K. 1997 Particle response in a planar sudden expansion flow. *Expl Thermal and Fluid Sci.* **15**, 413–423.

Fessler, J. R., Kulick, J. D. &. Eaton, J. K. 1994 Preferential concentration of heavy particles in a turbulent channel flow. *Phys. Fluids* **6**, 3742–3749.

Gore, R. A. & Crowe, C. T. 1991 Modulation of turbulence by dispersed phase. *J. Fluids Engng* **113**, 304–307.

Hardalupas, Y., Taylor, A. M. K. P. & Whitelaw, J. H. 1992 Particle dispersion in a vertical round sudden expansion flow. *Proc. R. Soc. Lond.* A **341**, 411–442.

Hetsroni, G. 1989 Particles-turbulence interaction. *Intl J. Multiphase Flow* **15**, 735–746.

Hishida, K., Ando, A., Hayakawa, A. & Maeda, M. 1989 Turbulence flow characteristics of dispersed two-phase flow in plane shear layer. In *Applications of Laser Anemometry to Fluid Mechanics* (ed. R. J. Adrian *et al.*). Springer.

Hishida, K. & Maeda, M. 1991 Turbulence characteristics of particle-laden flow behind a reward facing step. ASME FED, vol 121, pp. 207–212.

Kulick, J. D., Fessler, J. R. & Eaton, J. K. 1994 Particle response and turbulence modification in fully developed channel flow. *J. Fluid Mech.* **277**, 109–134.

Le, H. & Moin, P. 1994 Direct numerical simulation of turbulent flow over a backward-facing step. *Mech. Engng Dept. Rep.* TF-58. Stanford University, Stanford, California.

Longmire, E. K. & Eaton, J. K. 1990 Structure and control of a particle-laden jet. *Mech. Engng Dept. Rep.* MD-58. Stanford University, Stanford, California.

Maeda, M., Hishida, K. & Furutani, T. 1980 Optical measurements of local gas and particle velocity in an upward flowing dilute gas-solids suspension. In *Proc. Polyphase Flow and Transport Technology*, pp. 211–216. Century 2-ETC, San Francisco.

Maeda, M., Kiyota, H. & Hishida, K. 1982 Heat transfer to gas-solids two-phase flow in separated, reattached, and redevelopment regions. *Proc. 7th Intl Heat Transfer Conf.*, Munich (ed. U. Grigull, E. Hahne, K. Stephan & J. Strands). vol. 5, pp. 249–254. Hemisphere.

https://doi.org/10.1017/S0022112099005741 Published online by Cambridge University Press

Mostafa, A. A., Mongia, H. C., McDonell, V. G. & Samuelsen, G. S. 1989 On the evolution of particle-laden jet flows: A theoretical and experimental study. *AIAA J.* **27**, 167–183.

Rogers, C. B. & Eaton, J. K. 1991 The effect of particles on fluid turbulence in a flat-plate boundary layer in air. *Phys. Fluids* A **3**, 928–937.

Rouson, D. W. I., Eaton, J. K. & Abrahamson, S. D. 1997 A direct numerical simulation of a particle-laden turbulent channel flow. *Mech. Engng Dept Rep.* TSD-101. Stanford University, Stanford, California.

Simpson, R. L. 1996 Aspects of turbulent boundary layer separation. *Prog. Aerospace Sci.* **32**, 457–521.

Squires, K. D. & Eaton, J. K. 1990 Particle response and turbulence modification in isotropic turbulence. *Phys. Fluids* A **2**, 1191–1203.

Squires, K. D. & Eaton, J. K. 1994 Effect of selective modification of turbulence on two-equation models for particle-laden turbilent flows. *J. Fluids Engng* **116**, 778–784.

Stokes, G. G. 1851 On the effect of internal friction on the motion of a pendulum. *Trans. Camb. Phil. Soc.* **9**, 8–16 [Reprinted in 1922 *Mathematics and Physics Papers III*. Cambridge University Press].

Torobin, L. B. & Gauvin, W. H. 1959 Fundamental aspects of solid-gas flow. *Can. J. Chem Engng* **37**, 129–141.

Tsuji, Y. & Morikawa, Y. 1982 LDV measurements of an air-solid two-phase flow in a horizontal pipe. *J. Fluid Mech.* **120**, 385–409.

Tsuji, Y., Morikawa, Y. & Shiomi, H. 1984 LDV measurements of an air-solid two-phase flow in a vertical pipe. *J. Fluid Mech.* **139**, 417–434.

Yang, Y., Chung, J. N., Troutt, T. R. & Crowe, C. T. 1990 The influence of particles on the spatial stability of two-phase mixing layers. *Phys. Fluids* A **2**, 1839–1845.

https://doi.org/10.1017/S0022112099005741 Published online by Cambridge University Press